Frontier 1

Direct Observation of Vortices in Superconductors

by Using a Field-Emission Electron Microscope

Akira TONOMURA
Advanced Research Laboratory, Hitachi, Ltd.
Hatoyama, Saitama 350-0395, Japan
CREST, Japan Science and Technology Corporation
Kawaguchi, Saitama 332-0012, Japan

Abstract

A dissipation-free current can be obtained in a superconductor only when the tiny magnetic vortices,which penetrate a superconductor when a magnetic field is applied, are pinned down against the current-induced force. These vortices in superconductors have become dynamically observable by Lorentz microscopy using a 300-kV field-emission transmission electron microscope. As material defects can be observed while the vortices are being observed, the vortex pinning phenomena critical to the practical applications of superconductors can now be microscopically and dynamically observed.

1. Introduction

Vortices are closely related not only to the fundamentals of superconductors but also to their practical applications of superconductors. When we want to use a type II superconductor, for example, as a dissipation-free conductor of a large electric current, we need to keep vortices from moving due to the Lorentz force exerted on them by the current. Otherwise, the voltage difference induced by the movement of magnetic flux eventually breaks down superconductivity due to the dissipation. To increase the critical current at which vortices begin to move, we need to fix them in place. The mechanism of the vortex pinning, however, is not well understood because it is both microscopic and complicated. The efforts to develop practical superconducting materials with large critical currents have, therefore, largely been processes of trial and error.

The direct observation of the vortex behavior at pinning centers was a dream of electron microscopists for almost 40 years.[1-3], and was finally realized[4] by utilizing the phase information provided by a bright field-emission electron beam.[5-7]

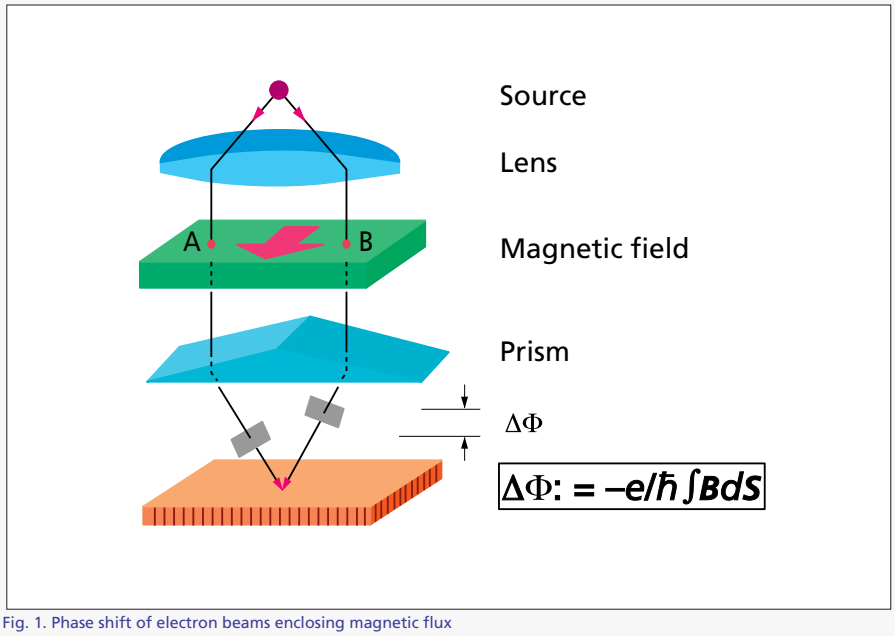

Fig. 1. Phase shift of electron beams enclosing magnetic flux
A relative phase shift between two electron beams starting from a source point, passing through points A and B in a magnetic field, and combining at an observation point is proportional to the magnetic flux enclosed by the two beam paths.

2. Observation Principle

The principle behind the observation of vortices is based on the use of the phase information of an electron wave transmitted through magnetic fields of vortices.[8] The phase shift of electron waves due to electromagnetic fields can be derived using the Schrödinger equation. When the effect of electromagnetic fields on electron waves is weak, the relative phase shift ΔS between two beams starting from the same point, passing through points A and B in electromagnetic fields $(\boldsymbol{A}, V)$, and combining at another point is calculated as follows.

$$\Delta S = (1/\hbar) \oint (m\boldsymbol{v} - e\boldsymbol{A})d\boldsymbol{s} = (1/\hbar) \oint (\sqrt{2meV} - e\boldsymbol{t}\boldsymbol{A})ds. \quad \cdots (1)$$

Here $\boldsymbol{t}$ is the unit tangent vector of the electron trajectory and the integration is carried out along a closed loop connecting the two electron trajectories. This equation shows that the phase shift in an electron beam is determined by electromagnetic potentials $(\boldsymbol{A}, V)$ rather than electromagnetic fields $(\boldsymbol{E}, \boldsymbol{B})$.

Aharonov and Bohm asserted that an electron beam can be affected physically (phase-shifted) by potentials even when it passes through field-free regions on both sides of an infinitely long solenoid and is therefore subjected to no forces.[9] This Aharonov-Bohm effect was confirmed by using toroidal ferromagnets.[10]

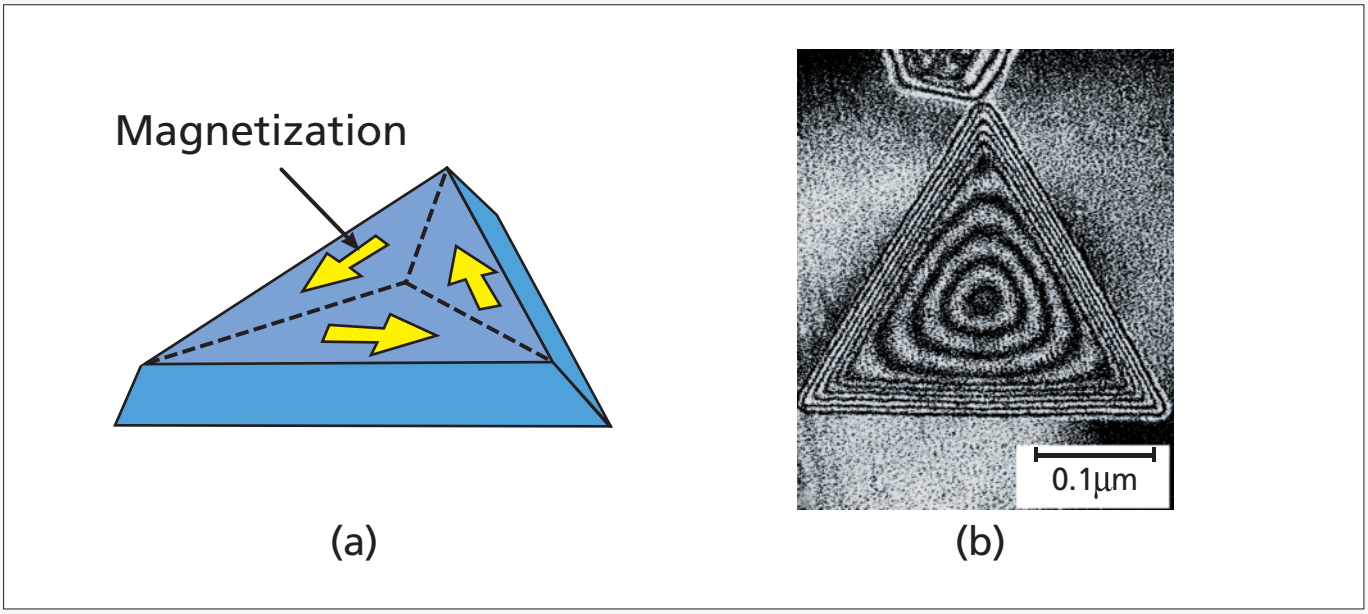

Fig. 2. Cobalt fine particle.
(a) Schematic diagram
(b) Interference micrograph
Only the triangular outline of this particle is observed by electron microscopy. Two kinds of contour fringes appear in its interference micrograph[8] : narrow fringes parallel to the edges indicate the thickness contours, and circular fringes in the inner region indicate in-plane magnetic lines of force.

This principle has been used to observe the microscopic distributions of electromagnetic fields. To be more specific, the thickness distribution of a specimen uniform in material can in principle be observed because the phase of an electron wave is shifted by the inner potential of the specimen when the wave passes through it. For thickness changes in the atomic range, though, the phase shift calculated from Eq. (1) is smaller than 2π. More precise measurements of the electron phase became feasible with the development of a "coherent" field-emission electron beam and electron holography.[8] In fact, thickness changes due to monatomic steps[11] and carbon nanotubes[12] have actually been detected as phase shifts of the order of 1/100 of 2π.

In the case of pure magnetic fields, the phase shift ΔS due to vector potentials can also be calculated from the magnetic flux Φ passing through the closed loop connecting the two trajectories:

$$\Delta S = -\frac{e}{\hbar} \oint \boldsymbol{A} d\boldsymbol{s} = -\frac{e}{\hbar} \int \boldsymbol{B} d\boldsymbol{S} = -\frac{e\Phi}{\hbar} \quad \ldots(2)$$

When the phase distribution due to magnetic fields is displayed as an interference micrograph obtained through the electron holography process,[8] it can be interpreted in the following straightforward way.

1. Contour fringes in the interference micrograph indicate magnetic lines of force, since there is no relative phase shift (ΔS) between two beams passing through two points along a magnetic line (see Fig. 1).
2. Contour fringes show magnetic flux in units of h/e, since the phase difference between two beams enclosing a magnetic flux of h/e is 2π.

Magnetic lines of force inside a ferromagnetic fine particle are shown in Fig. 2. Narrow fringes parallel to the edges indicate thickness contours. The circular fringes in the inner region indicate magnetic lines of force, since the thickness is uniform there.

Interference microscopy is not the only technique that can be used to visualize the phase distribution. For example, a phase object can be observed in an out-of-focus image because the phase change is transformed into an intensity change when the image is defocused. A vortex in a superconductor, which acts as a pure weak phase object to an illuminating electron beam, has been visualized as a black-and-white spot in a defocused image, or Lorentz micrograph.[4]

3. Observation of Vortices in Superconductors

Vortices can be detected by using the phase shift of an electron wave which interacts with the magnetic fields of the vortices.

3.1 Observation of magnetic lines of force of vortices leaking from the superconductor surface

A thin-film sample was prepared by evaporating lead onto a tungsten wire from one direction. A magnetic field perpendicular to the film was applied, and the sample was cooled to 4.5 K. Magnetic fields partially penetrating the film were observed in an electron-holographic interference micrograph by using an electron beam incident parallel to the film surface.

Interference micrographs[13] for film thicknesses of 0.2 μm and 1 μm are shown in Fig. 3. The lower black region in each micrograph is the shadow of the lead thin film, and the contour fringes above it correspond to the magnetic lines of force in flux units of $h/2e$, since the micrographs are phase-amplified by a factor of two. One fringe indicates the magnetic line of force of a single vortex. It can be seen from these two micrographs that the manner of magnetic field penetration varies for different thicknesses.

When the film is 0.2-μm-thick (Fig. 3(a)), isolated vortices can be seen. A magnetic line is produced from a region as narrow as 0.15 μm and fans out into the free space on the left side of the micrograph. A magnetic line form-

ing an arc is also seen on the right. It is a magnetic line connecting an antiparallel pair of vortices. This vortex and antivortex pair was presumably created by thermal excitation due to the Kosterlitz-Thouless transition and is thought to be frozen to be pinned.

Magnetic lines of force penetrate a thicker film not as individual vortices but as bundles of vortices. No vortex pairs are seen in Fig. 3(b). This can be interpreted as follows: when a strong magnetic field is applied to a thick film of lead, which is a type I superconductor, the film is divided into normal and superconducting domains (*intermediate state*). Magnetic lines of force can pass through normal regions. Since a normal region is surrounded by a superconducting region, the total flux is quantized to an integral multiple of $h/2e$. An extremely thin film, however, looks as if it were a type II superconductor.

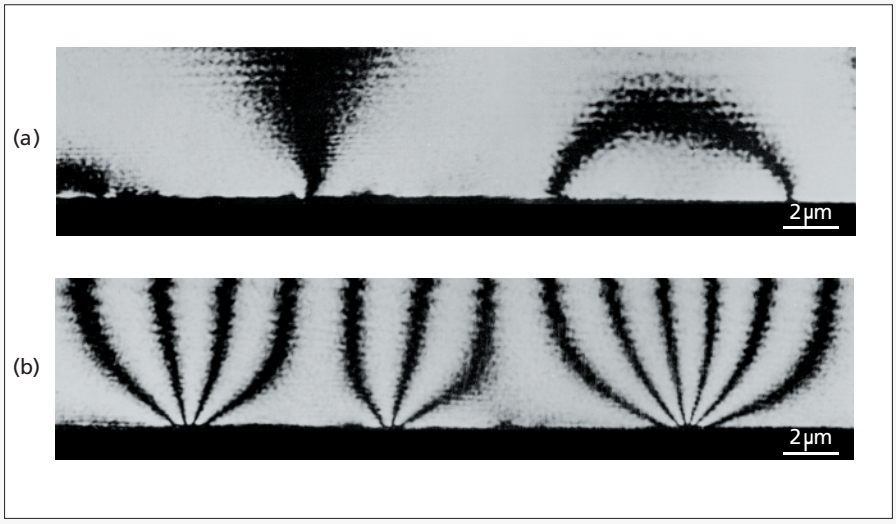

Fig. 3. Interference micrographs of magnetic lines of force leaking outside from vortices in a thin film of lead (phase amplification: A × 2).
(a) Film thickness = 0.2μm
(b) Film thickness = 1.0μm
One contour fringe corresponds to the magnetic flux of one vortex, or $h/2e$. Individual vortices penetrate the film thinner than 0.5μm (mixed state), but bundles of vortices penetrate the thicker film (intermediate state).

3.2 Observation of vortices inside superconductors

Vortices inside a superconductor can be observed when an electron beam passes through a thin-film sample.[14] The experimental arrangement for observing vortices in a superconductor is shown in Fig. 4. When a superconducting thin film is tilted and a magnetic field is applied horizontally, electrons passing through vortices in the film are phase-shifted, or deflected, by the magnetic fields of the vortices. Consequently, when the phase distribution is observed as an interference micrograph, projected magnetic lines of force can be observed.[15] However, by using this method it is not easy to observe dynamics of vortices. This can be done more easily by using Lorentz microscopy, in which vortices can be observed by simply defocusing the electron microscopic image. That is, when the intensity of electrons is observed in a out-of-focus plane, a vortex appears as a pair of bright and dark contrast features (Fig. 4).

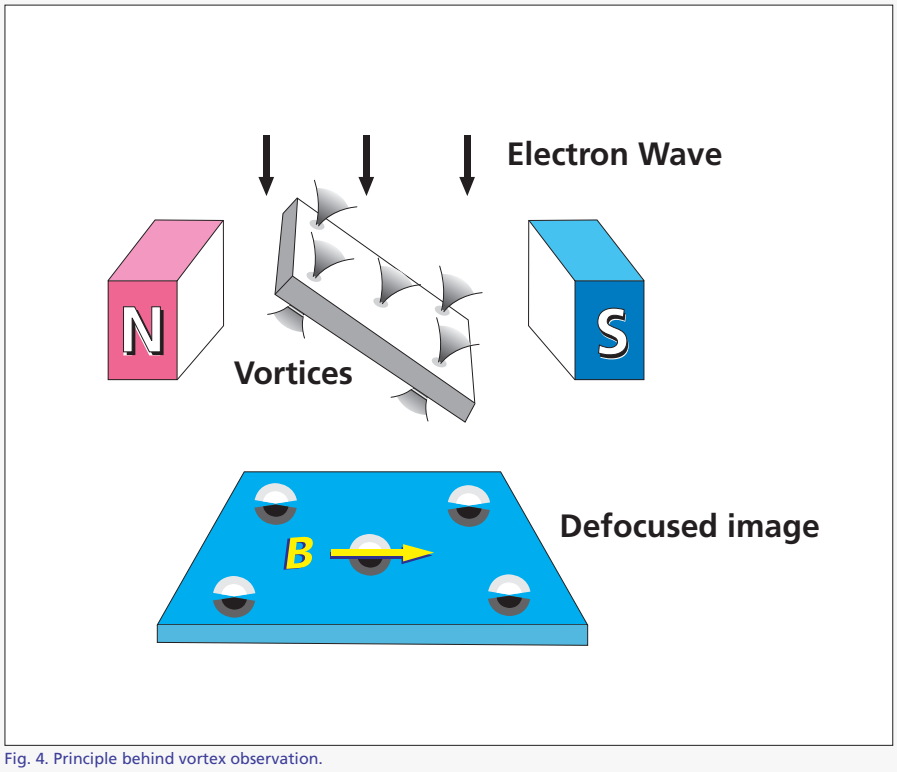

Fig. 4. Principle behind vortex observation.
An incident electron wave is phase-shifted, or deflected, by the magnetic fields of vortices. In the defocused image, a vortex appears as a spot consisting of black-and-white contrast (Lorentz microscopy).

A. Vortex depinning at different defects

Lorentz microscopy can reveal when and how vortices are depinned when a driving force is applied and increased. An example is shown in Fig. 5. Lines of point defects (black dots in Fig. 5) in a thin film of Nb were produced by irradiating it with a focused Ga-ion beam and changing the irradiation dose from line to line. The dependence of the pinning force on the ion doses producing the defects was investigated by observing behavior of the vortices when the driving force was increased by changing the applied magnetic field.

When a magnetic field of 100 G was applied, vortices were produced so close together that the vortices pinned at the defects could not be distinguished from unpinned vortices. When the magnetic field was decreased, only unpinned vortices began to leave the film but weakly pinned vortices also began to move: vortices hopped from one defect to another along a defect line as if they were jumping over stepping stones.

It can be seen from the Lorentz micrograph that all the unpinned vortices left the film during this experiment and that vortices pinned at defects produced by the ion irradiation with the dose of 1000 times larger than the unit dose did not move at all. No vortices remained trapped at defects produced by irradiation with less than 10 times the unit dose. For the defects produced by irradiation with 20- and 70 times doses, some of the pinned vortices were trapped at the defects depending on the ion dose.

If the critical current is to be increased, all the vortices have to be pinned. When there are many defects, vortices are pinned by them. Too many defects lead to the destruction of the superconductivity, but there are other factors influencing the vortex pinning effect. The interaction between vortices, for example, plays an important role in increasing critical current, especially when the magnetic field is strong.

B. Effect of vortex-vortex interaction on vortex pinning

When a weak magnetic field (< 7 G) was applied to a thin film of Nb containing widely spaced defects with fairly strong pinning forces (ion dose of 70 times the unit dose), vortices pinned at the defects did not begin to move easily, while unpinned vortices far from defects began to move freely. Vortices passing near the defects at which other vortices were pinned, however, were deflected by the magnetic repulsive force between the pinned vortices and the moving ones. Even unpinned vortices in general did not move smoothly but hopped from one point to another due to the existence of weak pinning centers inherent in Nb samples, making the chance of vortices to collide with the vortices trapped at the defects at a high speed. In that case, an additional vortex sometimes entered a defect. However, two trapped vortices were unstable since the defect radius (150 Å) was smaller than that of a vortex (300 Å) and consequently in a few seconds one escaped from the defect. On rare occasions, vortices were even bounced from the vortex trapped at a defect.

Very interesting phenomena were found to occur when vortices were densely packed. Vortices in general repel each other because of their magnetic fields. When they are squeezed by an external magnetic field, however, they tend to form a closely packed lattice. In a material containing strong pinning centers (e.g. defects), vortices cannot form a single lattice but instead form domains of lattices (Fig. 6).

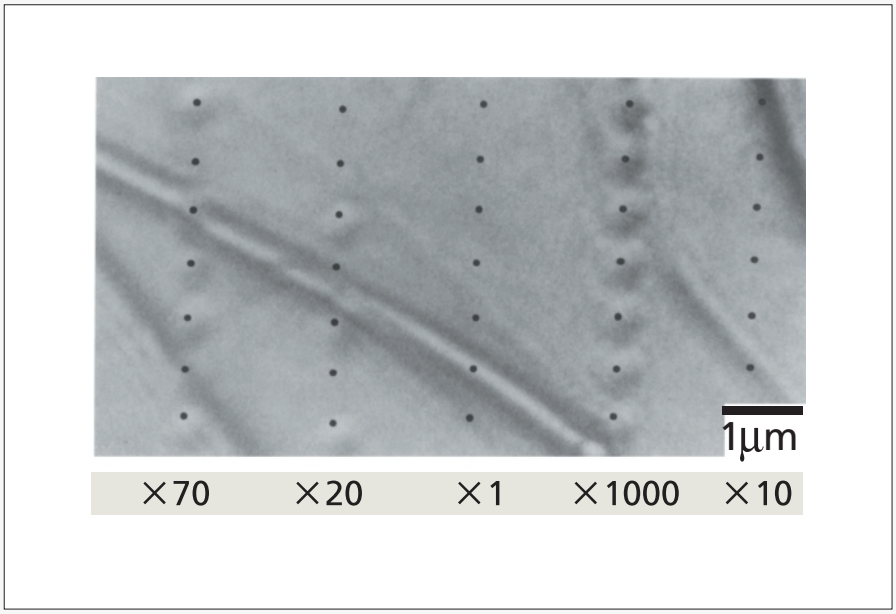

Fig. 5. Vortices trapped at lines of defects.
The numbers below the micrograph indicate the Ga-ion doses in units of 10^{-10} C. Vortices are trapped more strongly at defects produced by irradiation with larger doses.

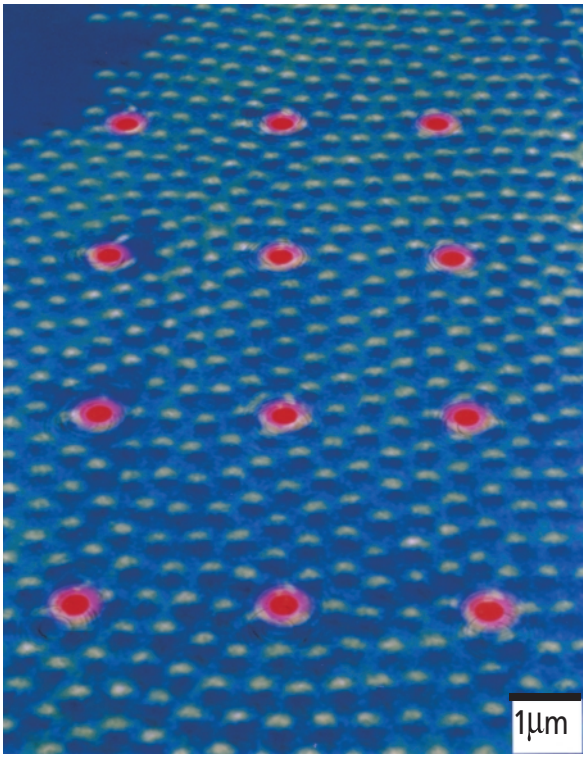

Fig. 6. Vortex configuration near artificial point defects.
Red spots indicate point defects produced by irradiation with a focused Ga-ion beam, and green spots indicate vortices. Vortices cannot form a single lattice since they are strongly trapped at the defects. When you look at this micrograph at a grazing angle, you can see domain boundaries of vortex lattices.

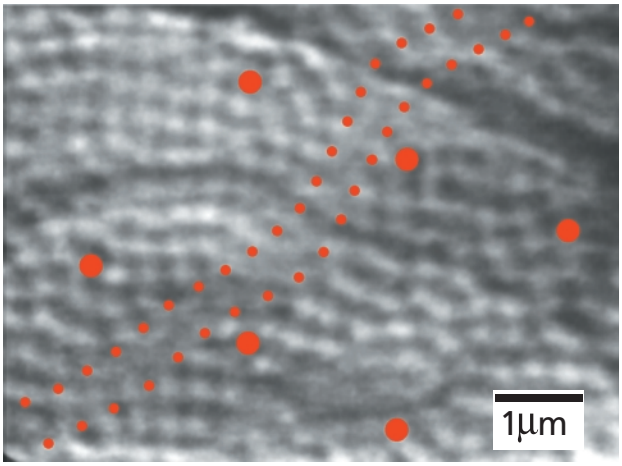

Fig. 7. Video frame during river flow.
When a driving force is exerted on vortices that form domains of lattices due to the existence of point defects, the vortices begin to flow in rivers along the domain boundaries. The images of vortices in the rivers are blurred because those vortices moved while this frame was being shot.

When a force was exerted on such a configuration of vortices and then increased, the vortices flowed intermittently along the domain boundaries.[16] Each defect strongly pinned not only a single vortex but also a domain of vortices. When the force reached a critical value, the weakest regions of the vortex configuration near the domain boundaries collapsed and vortices in those regions flowed in rivers.

A video frame of such a vortex river is shown in Fig. 7. The images of vortex inside the river are blurred because those vortices moved during the exposure time (1/30 sec) for one frame. This flow stopped in less than a second, forming a new domain structure. When the increasing force reached another critical value, they flowed again along new domain boundaries. This process was repeated, resulting in intermittent vortex rivers here and there. This was the first direct observation of vortices flowing in the form of plastic flows.[17], which was confirmed by numerical simulations made by Nori and his colleagues.[18, 19]

C. Peculiar vortex pinning in an array of pinning centers

The vortex pinning behaved completely differently when the pinning centers were densely arranged. This change in behavior occurred especially for a regular array of artificial point defects produced in a Nb thin film, where vortices formed regular and rigid configurations at specific values of magnetic fields. The net pinning force increased at these specific magnetic fields, which is known as the peak effect or the matching effect of the critical current, found by macroscopic measurements.

Lorentz micrographs showing the configurations of vortices relative to defect positions are shown in Fig. 8. At the matching magnetic field H_1 (Fig. 8(b)), all the defects are occupied by vortices and the lattice formed is a rigid square one. The peak effect of the critical current observed macroscopically can be explained microscopically: when vortices form a stable

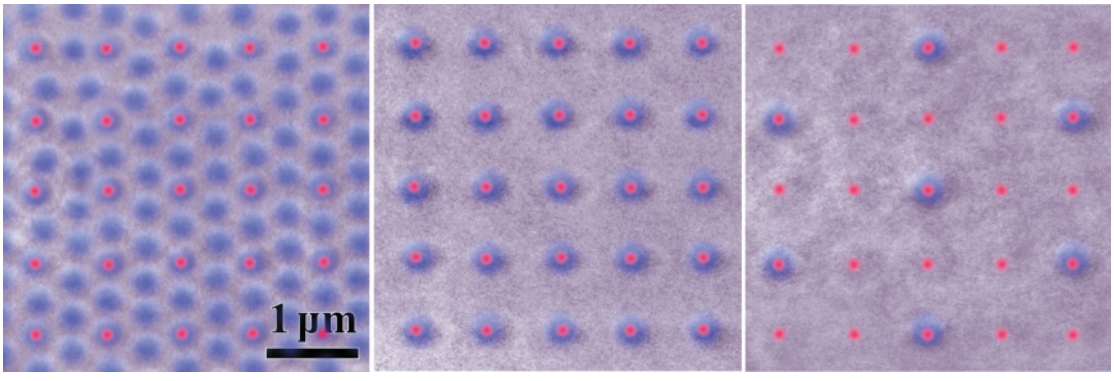

Fig. 8. Lorentz micrographs of vortices.
(a) $H = 4H_1$ (H_1: matching magnetic field)
(b) $H = H_1$
(c) $H = 1/4H_1$
Purple vortices form a regular and rigid lattice at these specific magnetic fields. If one of these vortices is thermally depinned from its red site by any chance, it cannot find a stable vacant site to hop to, thus producing a strong pinning effect.

and regular lattice without vacancies, even if a vortex is depinned from one pinning site due to thermal excitation, it can find no vacant site to move to. As a result, a stronger force is required to move the vortices.

Regular lattices were formed not only at $H = H_1$ (matching magnetic field, see Fig. 8(b)) but also at $H = mH_1/n$ (n and m; integers) as in the case of $H = 4H_1$ (Fig. 8(a)). In this vortex configuration, defect positions forming a square lattice were first occupied by vortices. Then two vortices aligned in the vertical direction were inserted at every interstitial site, and finally an additional vortex was inserted in the middle of two adjacent defects located vertically. Figure 8(c) shows the case at $H = 1/4H_1$. Vortices occupy every fourth site in the horizontal direction, thus forming a centered (4×2) rectangle lattice. The reason the pinning force as a whole becomes stronger at the specific values of magnetic fields comes from the fact that vortices form rigid and regular lattices.

When "excess" or "deficient" vortices were produced at magnetic fields different from the specific ones, such vortices could hop under a weaker force (see Fig. 9), just like "electrons" and "holes" that flow in a semiconductor. On the other hand, when a stronger force was applied to vortices forming a regular lattice, we observed a quite different flow of vortices such as a simultaneous movement of vortices along a lattice line.

D. Effect of antivortices on vortex pinning

We found unexpectedly during our observation experiments of vortices that antivortices were often produced and had a great influence on vortex pinning through the processes of creation and annihilation of antivortices.[20] This happened in commonplace processes, such as magnetization measurements. When the magnetic field applied to a Nb thin film was suddenly switched off, 90% of the vortices left the film instantly, 10% are pinned at weak pinning centers for a while, and then gradually left the film by hopping.

When the magnetic field was then applied in the opposite direction and gradually increased, the speed of the vortices increased. Before they left the film, however, antivortices appeared at the edges of the film and moved towards the inner region of the film. Where streams of vortices and antivortices collided head-on, the antiparallel pairs at the heads of the two streams annihilated each other.

Figure 10 shows two video frames, one just before the annihilation of such a pair and the other just after. When this pair annihilated each other, the next vortex and antivortex approached by hopping and annihilated each other. The results of macroscopic measurements, such as magnetization measurements of this state, provided no evidence of this phenomenon because the total magnetic flux in this field of view is zero as long as the sample contains equal numbers of vortices and antivortices. The annihilation process was revealed only when the vortices and antivortices were individually observed in real time.

Antivortices have a dramatic effect on vortex pinning in the case where strong pinning centers exist locally. In fact, when the magnetic field applied to a film was decreased, only the unpinned vortices left the film. Then, antivortices were produced from the film edges even though the magnetic field was not applied in the opposite direction. The produced antivortices approached the trapped vortices at the pinning centers, collided head-on with them and disappeared. The cause of the antivortices is as follows: the magnetic lines of a trapped vortex produced from the top surface of the film went the long way beyond the film edge and returned to the original vortex from the back surface. Therefore, the direction of the magnetic field was opposite at the film edge, thus producing antivortices at the edge.

The mutual annihilation of a trapped vortex and an incoming antivortex is equivalent to the depinning of the trapped vortex. Therefore when such an event occurs, the effective vortex depinning can take place easily.

E. Unconventional vortex movements in high-Tc superconductors

The critical current of high-Tc superconductors is, in general, very low because both the high temperature and the layered structure of the materials make it easy for vortices in them to move. When the vortex movement at the depinning threshold was investigated by gradually increasing the magnetic field applied to vortices in a high-Tc $Bi_2Sr_2CaCu_2O_{8+\delta}$(Bi-2212) superconductor, it was found that vortices moved in quite different manners depending on the applied magnetic field and the sample temperature.[21] In particular, the vortex movement above 25 K was quite different from that below this temperature.

Below 25 K all the vortices migrated slowly at almost the same speed (Fig. 11(a)). Their speed was 1.5 μm/s at 20 K, and decreased rapidly when the temperature was lowered. Above 25 K, however, vortices moved in different forms of plastic flow depending on the strength of the magnetic field. When it was

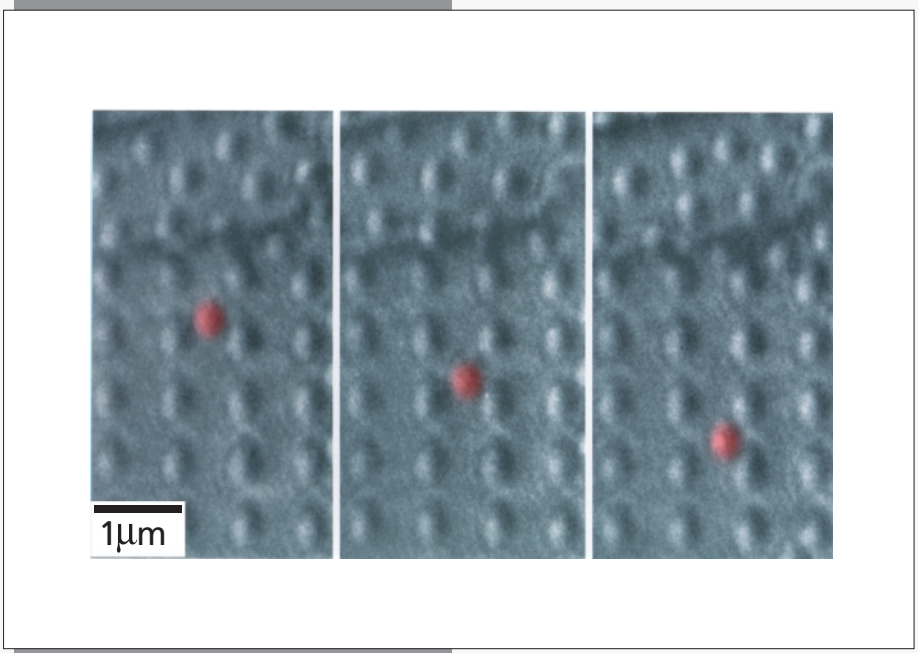

Fig. 9. Hopping interstitial vortex.
When the applied magnetic field is different from the specific values, "excess" or "deficient" vortices are produced and can easily hop from one site to another just like the "electrons" or "holes" in a semiconductor when a driving force is applied to them.

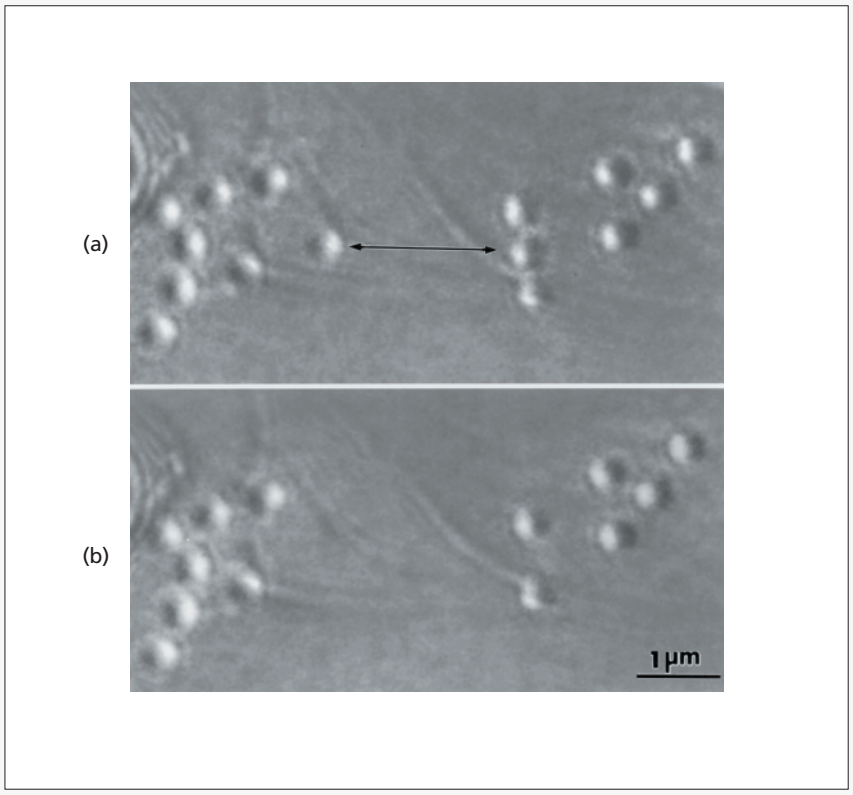

Fig. 10. Annihilation of vortices and antivortices in a thin film of niobium.
(a) Before annihilation
(b) After annihilation
When the magnetic field applied to the film is suddenly reversed, some vortices remain at weakly pinning defects while others begin to leave them. Antivortices begin to move in from the edges of the film. Where streams of vortices and antivortices collide head-on, the vortex-antivortex pairs of the heads of the two streams annihilate each other.

less than 1 G, the extremely sparse vortices trapped at preferential points suddenly hopped, one by one, from one point to another (Fig. 11(b)). The hopping was so frequent and sudden that the vortex image on video looked as if it were blinking on and off.

When the magnetic field was increased, the slow migration movement evident below 25 K remained the same but the individual hopping movement above 25 K changed. The forms of movement depended on how closely the vortices were packed, and such forms as filamentary flow, river flow, and lattice-domain flow were observed as the magnetic field increased.

This temperature-dependent change in the kinds of vortex movement seen in high-Tc superconductors can be interpreted as a result of vortices being pinned at extremely tiny defects, perhaps oxygen defects. The coherence length (the radius of the normal core of the vortex) is as small as 10Å in Bi-2212, whereas in niobium it is 300 Å. Therefore, below 25 K vortices are trapped by oxygen defects, which act as densely distributed pinning centers. Since a single vortex line penetrating a film 2000 Å thick may be collectively pinned by more than 100 oxygen defects, it would appear to move smoothly in the direction of the applied force.

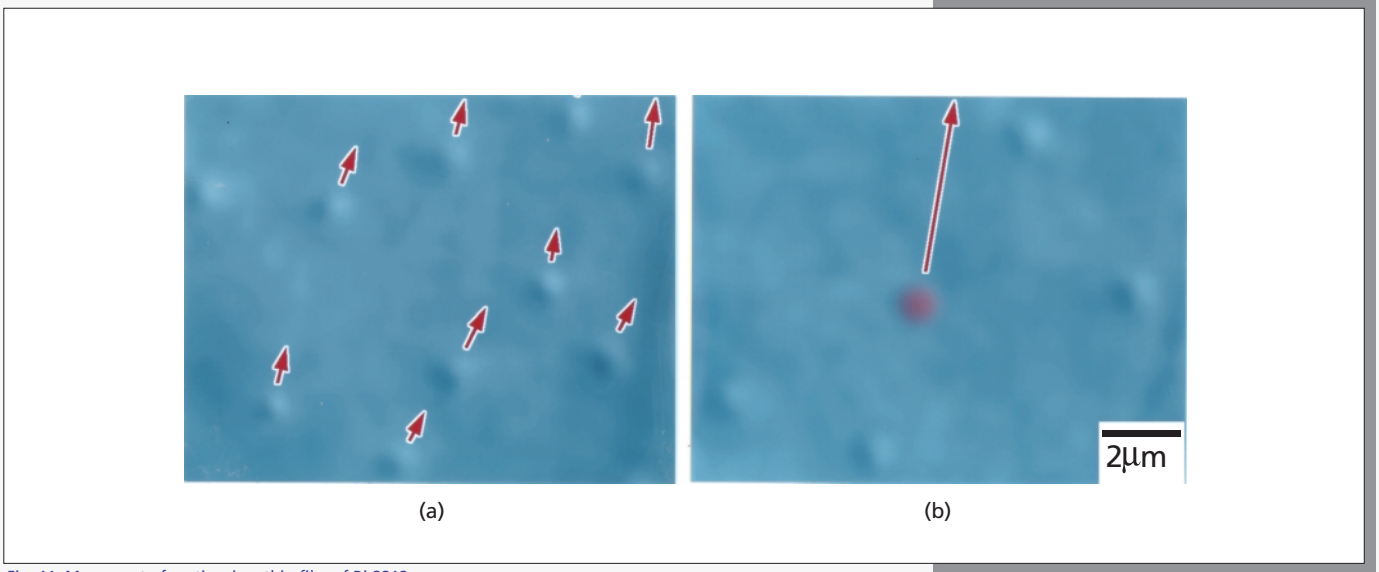

Fig. 11. Movement of vortices in a thin film of Bi-2212
(a) Migration movement below 25 K
(b) Hopping movement above 25 K
At temperatures below 25 K a single vortex line is collectively pinned by a great number of oxygen defects and migrates slowly, assisted by thermal activation, when a driving force is applied. Above 25 K the oxygen defects no longer have a pinning effect strong enough to withstand the increased thermal vibration of the vortices, and the pinning effect at larger defects, which predominates at higher temperatures, results in hopping movement.

This is because the thermally activated vortex line would begin to be depinned from these defects one by one on one side of the line and to become pinned at new defects on the other side. This would result in a migration that resembles the movement of an object through a viscous fluid.

Increased thermal vibration, however, causes the vortices to be easily depinned from small defects, and above 25 K the pinning effect of the oxygen defects practically vanishes. The pinning at other larger and sparser defects, which below 25 K is hidden by the strong pinning at oxygen defects, predominates above 25 K because the pinning at larger defects is less influenced by thermal vibration.

Since these larger defects are distributed more sparsely, vortices depinned from one defect hop to another. When vortices become more abundant and form a closely packed lattice, it becomes difficult for them to move individually. The specific forms of movement are determined by the competition between random pinning forces and vortex-vortex forces.

4. Conclusion

Vortices in superconducting thin films were directly observed by monitoring the phase of an electron beam passing through them. This became possible after a bright electron beam and phase-imaging techniques were developed. The microscopic mechanism of vortex pinning was investigated by using these techniques to observe vortices depinned from material defects by applying an increasing force. A 1000 kV field-emission transmission electron microscope[22] has just been developed (Fig.12) and will be used to explore many interesting features of vortices in high-Tc superconductors. Applications of this new microscope are not limited to superconductivity. A bright electron beam having an extremely short wavelength will bring to the nanoscopic region in science and technology new possibilities, especially in high-precision measurements and in fundamental experiments in quantum mechanics, just as other bright sources such as synchrotron radiation sources and neutron sources now do.

JSAP

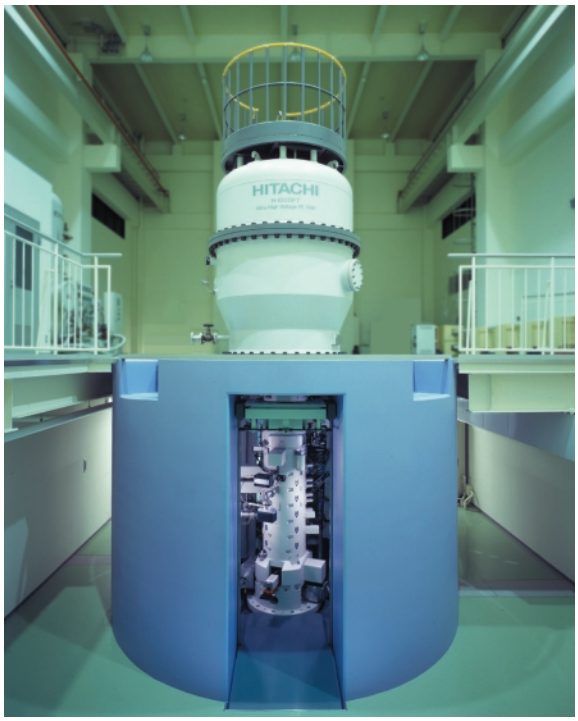

Fig. 12. 1000-kV field-emission transmission electron microscope.

References

1) H. Yoshioka: J. Phys. Soc. Jpn **21**, 948 (1966).
2) D. Wohlleben: J. Appl. Phys. **38**, 3341 (1967).
3) C. Colliex, B. Jouffrey and M. Kleman: Acta Crystallogr. A**24**, 692 (1968).
4) K. Harada, T. Matsuda, J. Bonevich, M. Igarashi, S. Kondo, G. Pozzi, U. Kawabe and A. Tonomura: Nature **360**, 51 (1992).
5) A. V. Crewe, D. N. Eggenberger, D. N. Wall and L. N. Welter: Rev. Sci. Instrum. **39**, 576 (1968).
6) A. Tonomura, T. Matsuda and J. Endo: Jpn. J. Appl. Phys. **18**, 9 (1979).
7) T. Kawasaki, T. Matsuda, J. Endo and A. Tonomura: Jpn. J. Appl. Phys. **29**, L5089 (1990).
8) A. Tonomura: Electron Holography - 2nd Edition, Springer, Heidelberg (1999).
9) M. Peshkin and A. Tonomura: Lecture Notes in Physics, **340** (Springer-Verlag, 1989).
10) A. Tonomura, N. Osakabe, T. Matsuda, T. Kawasaki, J. Endo, S. Yano and H. Yamada: Phys. Rev. Lett. **56**, 792 (1986).
11) A. Tonomura, T. Matsuda, T. Kawasaki, J. Endo and N. Osakabe: Phys. Rev. Lett. **54**, 60 (1985).
12) Q. Ru, G. Lai, K. Aoyama, J. Endo and A. Tonomura: Ultramicroscopy **55**, 209 (1994).
13) T. Matsuda, S. Hasegawa, M. Igarashi, T. Kobayashi, M. Naito, H. Kajiyama, J. Endo, N. Osakabe, A. Tonomura and R. Aoki: Phys. Rev. Lett. **62**, 2519 (1989).
14) T. Hirayama, N. Osakabe, Q. Ru, T. Tanji and A. Tonomura: Jpn. J. Appl. Phys. **34**, 3294 (1995).
15) J. E. Bonevich, K. Harada, T. Matsuda, H. Kasai, T. Yoshida, G. Pozzi and A. Tonomura: Phys. Rev. Lett. **70**, 2952 (1993).
16) T. Matsuda, K. Harada, H. Kasai, O. Kamimura and A. Tonomura: Science **271**, 1393 (1996).
17) G. W. Crabtree and D. R. Nelson: Phys. Today April, 38 (1997).
18) C. Reichhardt, J. Groth, C. J. Olson, S. B. Field and F. Nori: Phys. Rev. B **54**, 16108 (1996).
19) C. Reichhardt, C. J. Olson and F. Nori: Phys. Rev. Lett. **78**, 2648 (1997).
20) K. Harada, H. Kasai, T. Matsuda, M. Yamasaki and A. Tonomura: J. Electron Microsc. **46**, 227 (1997).
21) A. Tonomura, H. Kasai, O. Kamimura, T. Matsuda, K. Harada, J. Shimoyama, K. Kishio and K. Kitazawa: Nature **397**, 308 (1999).
22) T. Kawasaki, T. Yoshida, T. Matsuda, N. Osakabe, A. Tonomura, I. Matsui and K. Kitazawa: Appl. Phys. Lett. **76**, 1342 (2000).